# Rapid determination of ETS markers with a prototype field-portable GC employing a microsensor array detector

Qiongyan Zhong,[a] Rebecca A. Veeneman,[b] William H. Steinecker,[b] Chunrong Jia,[a] Stuart A. Batterman[a] and Edward T. Zellers*[ab]

*Received 8th January 2007, Accepted 12th March 2007*
*First published as an Advance Article on the web 2nd April 2007*
**DOI: 10.1039/b700216e**



The adaptation of a portable gas chromatograph (GC) prototype with several unique design features to the determination of vapor-phase markers of environmental tobacco smoke (ETS) is described. This instrument employs a dual-stage adsorbent preconcentrator, two series-coupled separation columns that can be independently temperature programmed, and a detector consisting of an array of nanoparticle-coated chemiresistors, whose response patterns are used together with retention times for vapor recognition. An adsorbent pre-trap was developed to remove semi-volatile organics from the sample stream. Conditions were established to quantitatively capture two ETS markers, 2,5-dimethylfuran (2,5-DMF) and 4-ethenylpyridine (4-EP, as a surrogate for 3-EP), and to separate them from the 34 most prominent co-contaminants present in ETS using ambient air as the carrier gas. A complete analysis can be performed every 15 min. Projected detection limits are 0.58 and 0.08 ppb for 2,5-DMF and 4-EP, respectively, assuming a 1 L sample volume, which are sufficiently low to determine these markers in typical smoking-permitted environments.

## Introduction

Environmental tobacco smoke (ETS) is a complex mixture of compounds collectively classified by the International Agency for Research on Cancer as a carcinogenic substance.[1] The complexity of ETS and the presence of confounding sources of some ETS constituents in many environments have impeded accurate exposure assessments and have led to efforts to find surrogate measures of ETS.[2] Vapor-phase nicotine (VPN) is the most widely used marker of ETS, but it is not ideal because of its low volatility and unpredictable decay rate.[3] A pyrolysis product of nicotine, 3-ethenylpyridine (3-EP), has been reported as an alternative ETS marker.[3,4] Concentrations of 3-EP correlate better with ETS particle concentrations and other gas-phase ETS components than do those of VPN, it is found exclusively in the vapor-phase, and its decay follows first-order kinetic models. Average concentrations of 3-EP measured in indoor environments where smoking is permitted typically range from 0.8–6.3 μg $m^{-3}$ (0.18–1.5 ppb), with average personal exposure levels generally somewhat lower (0.4–0.7 ppb). Exposures rarely exceed 4.5 ppb.[5–9]

Another compound, 2,5-dimethylfuran (2,5-DMF), has also been identified as a vapor-phase marker of ETS.[10,11] In tests designed to simulate ETS levels in an office environment, 2,5-DMF concentrations were found to range from 2.4–30 μg $m^{-3}$ (0.6–7.5 ppb).[10,11] Concentrations of 2,5-DMF in the breath of passively exposed non-smokers averaged 6.8 ppb, while those in the breath of smokers averaged 94 ppb immediately after smoking.[11]

The most widely reported methods for determination of 3-EP in indoor air entail sorbent-tube sampling followed by GC-MS or GC-NPD analysis.[6,8,9,12] Similarly, samples of 2,5-DMF vapor can be captured by canister or on Tenax-TA adsorbents and analyzed by GC-MS.[10,11] Although such methods are undoubtedly reliable, the availability of portable instrumentation capable of monitoring ETS markers *in situ* would facilitate exposure assessments and interventions by allowing a greater number of measurements to be collected at lower cost and much higher temporal resolution, as well as providing immediate feedback to affected populations. Unfortunately, relatively few portable instruments are available with the capability for analyzing the components of complex vapor mixtures,[13–19] and the cost, complexity, and/or size of those with such capabilities preclude their use for extended or routine monitoring campaigns. Although Gordon *et al.* have described a fieldable breath analyzer,[11] there are no published reports on the determination of ambient concentrations of vapor-phase ETS markers with portable direct-reading instrumentation.

This article describes the adaptation of a prototype instrument for the determination of ETS markers in synthetic air samples also containing the major co-contaminants encountered in environments where smoking is permitted. An enhanced version of an earlier prototype,[20,21] this instrument uses scrubbed ambient air as the carrier gas to avoid the need for on-board gases, and incorporates a multi-stage adsorbent preconcentrator/focuser (PCF), a tandem-column separation module with independent 'at-column' temperature-programming capabilities and mid-point pressure/flow control, and a

[a] *Department of Environmental Health Sciences, University of Michigan, 109 S. Observatory, Ann Arbor, MI 48109-2029, USA. E-mail: ezellers@umich.edu*
[b] *Department of Chemistry, University of Michigan, Ann Arbor, MI, USA*

 

detector comprising an array of microfabricated chemiresistor (CR) sensors with nanoparticle interface layers.

In this study, air samples were collected from a local bowling alley where smoking is allowed and analyzed by conventional methods to identify and quantify the two ETS markers, 2,5-DMF and 3-EP, and the major co-contaminants. Mixtures of these were then generated in the laboratory and conditions were established for the determination of the markers using a combination of retention times and the response patterns obtained from the CR array detector. Since at the outset of the study 3-EP was not commercially available, its isomer, 4-EP, was used as a surrogate.[12] A pre-trap was developed for removing semi-volatile organic compounds (SVOCs) from the sample. Preconcentration factors and desorption efficiencies for the ETS markers were verified and chromatographic conditions were established to separate the markers from other contaminants in the shortest possible time. Using Monte Carlo simulations coupled with pattern recognition analysis of sensor array responses, it was possible to determine the degree of discrimination achievable between the markers and possible co-eluting interferences, and to use this information to accelerate the analysis.

## Experimental

### Instrument features and operating modes

Fig. 1 shows the layout of the analytical sub-system. Air flow provided by the on-board mini-pumps is directed through the required paths by a set of solenoid actuated valves with Teflon-wetted surfaces. The instrument has a footprint about twice that of a laptop computer, measuring 61 cm (l) ×33 cm (w) ×15 cm (h), and was constructed by Microsensor System, Inc., Bowling Green, KY, USA, according to a mutually determined set of specifications. A detailed description of the instrument components and the rationale for the design will be provided elsewhere.[22]

The instrument has three operating modes. In sampling mode, air is drawn through the pre-trap and the PCF at 0.13 L $min^{-1}$ by the sampling pump. Vapors not removed by the pre-trap (see below) are captured on one of the two PCF adsorbents contained in an insulated Inconel 600® tube (1.35 mm i.d., 5 cm long). The PCF tube was packed, in order, with 3 mg each of 40/60 mesh Carbopack X and Carbopack B (separated by glass wool), which have specific surface areas of 250 $m^2$ $g^{-1}$ and 100 $m^2$ $g^{-1}$, respectively (Supelco, Bellefonte, PA, USA).[23] After sampling a pre-determined air volume, typically 1 L for this study, the sampling pump is turned off and isolated from the system by an upstream valve (Fig. 1(a)). An optional purge mode can be included during which the analysis pump draws ambient air in through a second inlet port and passes it through a scrubber cartridge packed with molecular sieves and charcoal to remove water vapor and VOCs. The purified air passes through the PCF (at room temperature) to strip a portion of the water vapor from the adsorbents and to backflush it, along with any residual contaminants in the fore line, out through the sample inlet port. In analysis mode, the PCF is heated (*via* an insulated copper wire coil) to 300 °C in <2 s and maintained at this temperature for

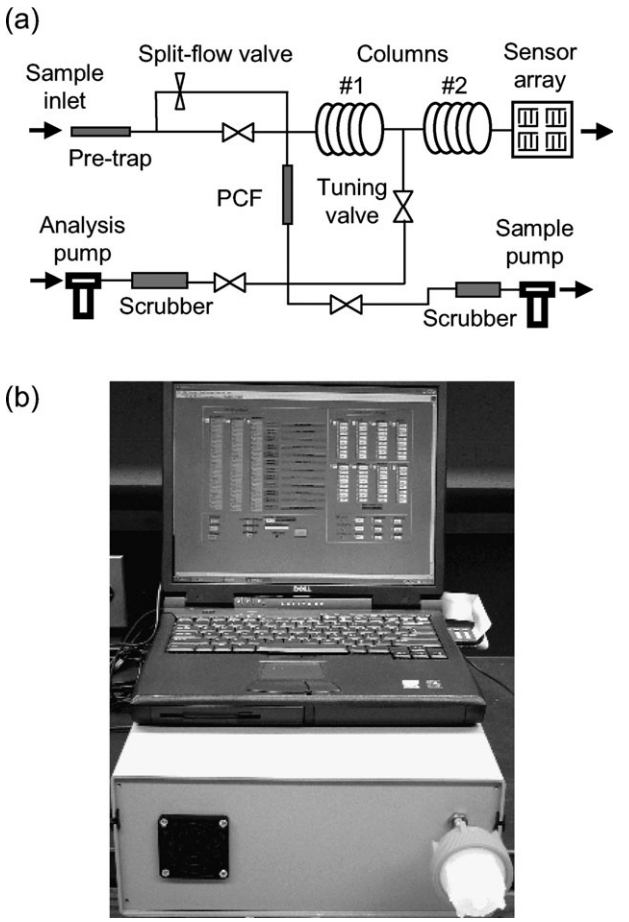


**Fig. 1** (a) Schematic of fluidic sub-system and (b) photograph of the prototype instrument beneath a laptop computer (PCF = preconcentrator/focuser).

90 s. Ambient air drawn into the system by the analysis pump is scrubbed, as in purge mode, and then directed through the PCF, the two separation columns, and the detector cell containing the sensor array prior to exiting the instrument. Desorbed vapors are thereby injected onto the first of the two separation columns, with the option of splitting off a portion of the desorbed flow stream (by opening the split-flow control valve) for the purposes of sharpening the injection band.

Each fused-silica capillary column is 4.5 m long (0.25 mm i.d.). The first has a nonpolar polydimethylsiloxane bonded stationary phase (DB-1, 0.5 μm thickness, Agilent, Wilmington, DE, USA) and the second has a bonded phase of moderately polar polytrifluoropropylmethylsiloxane (RTX-200, 0.25 μm thickness, Restek, Bellefonte, PA, USA), which has retention properties complementary to those of the DB-1 column. The columns are heated independently using coiled 'at-column' heaters.[20,24] A bypass line shunts flow around the first column when the tuning valve is open, which stops the flow in the first column while accelerating the flow through the second column. This valve can be opened for short periods of time during an analysis to separate compounds that are resolved on the first column but re-converge at the end of the second column.[20,21,25]

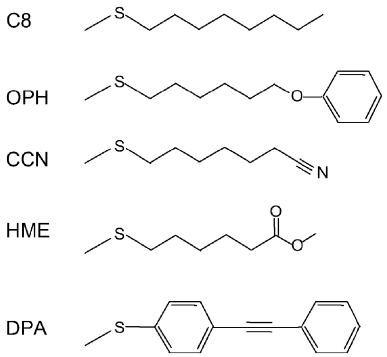


**Fig. 2** Structures of the thiolate monolayers on the MPNs.

Eluting vapors are recognized and quantified by the CR array, which consists of four sets of interdigital Au/Cr electrodes patterned on a single oxide-coated Si substrate. Each CR sensor is coated with a different gold–thiolate monolayer protected nanoparticle (MPN).[26,27] The coated array is capped with a Macor® lid (cell volume ~3 μL) and fitted with inlet and outlet capillaries for fluidic interconnections. MPNs derived from the following thiols were used in this study: *n*-octanethiol (C8), 1-mercapto-6-phenoxyhexane (OPH), 7-mercaptoheptanitrile (CCN), methyl 6-mercaptohexanoate (HME), and 4-mercaptodiphenylacetylene (DPA).[28] The structures of the thiolates are presented in Fig. 2. The CR array is mounted on a custom PC board using soldered pins and a matching socket. A constant DC bias is applied to each sensor and the current is converted to a voltage, baseline corrected, amplified, and transmitted to a D/A card on a laptop computer. The baseline voltage is determined by the value of the reference (feedback) resistor placed in series with each sensor.

In the CR array, vapors reversibly partition into each MPN film and cause it to swell, which changes the electron tunneling barrier and thereby the film resistance.[29] Since the structures of the MPN ligands differ on each sensor, the affinities for a given vapor differ as well, and the array of CRs produces a different set of responses for each vapor. The pattern of responses can then be combined with the retention time to identify each vapor, and the magnitudes of the responses from the sensors can be used collectively to quantify the vapor concentrations.[21,26,27] Following detection, the PCF and pre-trap are re-conditioned by sequentially heating and purging with scrubbed air, and then cooling actively with on-board fans prior to collecting the next sample.

Software written in Labview® 7.1 (National Instruments, Austin, TX, USA) is run from a laptop computer and used to control the instrument and process the sensor output signals through separate 12 bit and 16 bit D/A data acquisition cards. Sensor output data are imported to Grams 32 (Thermogalactics, Salem, NH, USA) for peak integration.

### Field samples

Air samples from a local bowling alley were collected and analyzed on two different occasions using EPA Method TO-17.[30] The GC-MS (Model 6890-5973, MS in scan mode, Agilent, Palo Alto, CA, USA) was calibrated with 96 VOCs selected on the basis of their adverse health effects and prevalence as contaminants in indoor air.[31] Neither 3-EP nor VPN were included in this initial calibration library. They were added prior to analyzing samples from the second set of samples collected from the bowling alley.

### Test atmosphere generation

Chemicals were obtained from Aldrich (Milwaulkee, WI, USA), Acros/Fisher (Pittsburgh, PA, USA), or Lancaster (Windham, NH, USA) at ≥ 98% purity. Since 3-EP could not be obtained commercially, its isomer 4-ethenylpyridine (4-EP) was used. These isomers are reported to have the same GC retention time (and similar MS fragmentation patterns),[12] consistent with their similar vapor pressures, reported to be 1.70 torr for 4-EP[32] and estimated to be 1.65 torr for 3-EP on the basis of its boiling point.[33,34] Test atmospheres of the vapors were generated in clean, dry air from a compressed-air cylinder over a range of concentrations in a series of Tedlar® bags (25 ± 2 °C), and concentrations were compared to those determined using $CS_2$ solutions of the analytes by GC-FID (Model 6890, Agilent).

### Adsorbent-bed capacities and desorption efficiencies

A series of experiments was performed to identify the types and quantities of adsorbents for use in the pre-trap and PCF. The 10% breakthrough volume, $V_{b10}$, was determined by drawing a vapor sample through the adsorbent bed at 0.1 L $min^{-1}$, periodically collecting aliquots downstream in a 0.25 mL sample loop, and injecting *via* a 6-port valve into the GC-FID.[35] Desorption efficiencies were determined by injecting a known concentration of analyte(s) in air into a clean air stream being drawn through the adsorbent bed, reversing the flow and heating the adsorbent to 300 °C to inject the captured analytes into the GC-FID. Responses were compared to those for an equivalent mass injected directly to the GC-FID.

Instrument responses to relevant vapors were then compared with and without the pre-trap installed. The sample inlet was connected to one port of a 6-port valve and a miniature diaphragm pump (KNF Neuberger, Trenton, NJ, USA) was used to draw samples at 0.13 L $min^{-1}$ from a test atmosphere through a sample loop, on a background of scrubbed air. The PCF was then heated and the desorbed vapors injected into the separation module. The PCF and pre-trap were re-conditioned after each analysis by sequentially heating them to 300 °C while backflushing with clean air.

### Instrument calibration

The most prominent co-contaminants found to bracket 2,5-DMF and 3-EP in chromatograms obtained from field samples were divided into three subsets for calibration. Conditions required to separate the markers in a minimum amount of time were established. Sample loops with volumes ranging from 0.010–1 mL were used to cover the desired range of injected masses. Effective (mass-equivalent) vapor concentrations were calculated according to the ratio of injection and sample volumes. For example, an aliquot of 1 mL from

 

a sample loop containing 100 ppm of vapors is equivalent to 100 ppb in a sample volume of 1 L. Mass-equivalent calibration concentrations ranged from 0.15–150 ppb L. Five replicates were performed for each challenge concentration.

### Chemometrics

Chemometric analyses of sensor array response patterns were performed using extended disjoint principal components regression (EDPCR).[36,37] Expected recognition rates for the components of co-eluting mixtures were estimated by combining Monte Carlo simulations with EDPCR. The Monte Carlo simulations superimpose random error on calibrated sensor array response patterns, which are then analyzed by EDPCR to determine if the components giving rise to the composite response pattern can be determined with low error.[37] Iterative analysis ($n$ = 500) over a range of concentrations yield statistical estimates of discrimination.

## Results and discussion

### Contaminant profiles from field samples

GC-MS analysis of the first set of field samples collected from the bowling alley yielded more than 100 detectable peaks, 35 of which could be identified as among those in the initial spectral library used for identification (Table 1). These target compounds accounted for 44% of the collected mass (using toluene-equivalent mass for the unidentified fraction). Concentrations ranged from 0.06 ppb (*sec*-butylbenzene) to 50 ppb (toluene). The concentration of 2,5-DMF was 0.56 ppb. Since 3-EP was not included in the calibration library for this analysis, its presence and concentration could not be verified.

Subsequently, GC conditions were adjusted, the spectral library augmented, and a second set of field samples was collected, in this case from an area within the bowling alley with a greater number of active smokers. A total of 40 compounds (60% of VOC mass) were identified at concentrations of 0.061 ppb (*n*-butylbenzene) to 29 ppb (*d*-limonene). Table 1 presents the average concentrations (RSD < 20% for most vapors). The concentrations of 2,5-DMF and 3-EP were 1.2 and 2.0 ppb, respectively. VPN was also found in these samples; however, it could not be accurately quantified because of variable desorption efficiencies observed in experiments with VPN-spiked adsorbent tubes. As shown in Table 1, the VOC profiles are quite consistent between the two sampling campaigns.

**Table 1** Average concentrations (ppb) of ETS markers and co-contaminants found in a local bowling alley using EPA TO-17[a]

| No. | Compound | $p_v$/torr | Field set 1 (ppb) | Field set 2 (ppb) |
|---|---|---|---|---|
| 1 | Chloroform | 197 | nd | 0.24 |
| 2 | 1,1,1-Trichloroethane | 124 | 1.1 | 2.1 |
| 3 | Benzene | 95.2 | 2.1 | 4.0 |
| 4 | Ethyl acetate | 93.7 | nd | 16 |
| 5 | Carbon tetrachloride | 91 | 0.085 | 0.1 |
| 6 | Trichloroethylene | 69 | 1.5 | 1.7 |
| 7 | Methylcyclohexane | 46 | 1.2 | 0.75 |
| 8 | Toluene | 28.4 | 50 | 13 |
| 9 | 2,5-Dimethylfuran | 25.9 | 0.56 | 1.2 |
| 10 | Methyl isobutyl ketone | 19.9 | 2.6 | 1.1 |
| 11 | Tetrachloroethylene | 13 | 0.78 | 1.2 |
| 12 | *n*-Octane | 10.9 | nd | 1.1 |
| 13 | Ethylbenzene | 9.6 | 1.2 | 1.5 |
| 14 | *p*-Xylene | 8.8 | 3.7 | 4.2 |
| 15 | *m*-Xylene | 8.3 | | |
| 16 | *o*-Xylene | 6.6 | 1.1 | 1.2 |
| 17 | Styrene | 6.4 | 4.0 | 4.1 |
| 18 | α-Pinene | 4.8 | 0.61 | 0.83 |
| 19 | *n*-Nonane | 4.45 | 0.94 | 1.2 |
| 20 | Isopropylbenzene | 3.5 | 0.16 | 0.12 |
| 21 | *n*-Propylbenzene | 3.4 | 0.78 | nd |
| 22 | 4-Ethyltoluene | 3 | 4.0 | 1.1 |
| 23 | 2-Ethyltoluene | 2.6 | 1.0 | 0.47 |
| 24 | 1,3,5-Trimethylbenzene | 2.5 | 1.1 | 0.42 |
| 25 | 1,2,4-Trimethylbenzene | 2.1 | 3.8 | 1.3 |
| 26 | *d*-Limonene | 1.98 | 29 | 29 |
| 27 | *sec*-Butylbenzene | 1.75 | 0.060 | nd |
| 28 | 1,2,3-Trimethylbenzene | 1.7 | 0.73 | 0.67 |
| 29 | 3-Ethenylpyridine | 1.65[b] | nd | 2.0 |
| 30 | *p*-Isopropyltoluene | 1.46 | 0.19 | 0.52 |
| 31 | *n*-Decane | 1.4 | 3.3 | 1.6 |
| 32 | *n*-Butylbenzene | 1.06 | nd | 0.061 |
| 33 | 1,4-Dichlorobenzene | 1.0 | 7.5 | 6.9 |
| 34 | *n*-Undecane | 0.41 | 6.6 | 1.3 |
| 35 | Phenol | 0.35 | nd | 1.5 |
| 36 | *n*-Dodecane | 0.14 | 4.3 | 1.1 |
| 37 | Naphthalene | 0.085 | 0.14 | 2.1 |
| 38 | *n*-Tridecane | 0.0558 | 0.98 | 0.47 |
| 39 | Nicotine | 0.038 | nd | nq |
| 40 | *n*-Tetradecane | 0.0116 | 0.73 | 0.62 |
| 41 | *n*-Pentadecane | 0.00343 | 0.72 | 0.76 |
| 42 | *n*-Hexadecane | 0.00143 | 0.56 | 0.61 |

[a] Vapor pressure at 25 °C from ref. 32; nd = not detected; nq = detected but not quantified. [b] See text.

### Pre-trap

An adsorbent pre-trap was developed in order to minimize accumulation of SVOCs within the instrument. VPN ($p_v$ = 0.038 torr) was the most volatile and most polar of the SVOCs detected during field sampling, and was therefore chosen as the sentinel 'cutoff' vapor for assessing pre-trap capacity. A 2 mg bed of the lower surface area graphitized carbon, Carbotrap C (10 $m^2$ $g^{-1}$, 20/40 mesh, Supelco) challenged (0.1 L $min^{-1}$) in individual tests with ~450 ppb of VPN or 4-EP gave $V_{b10}$ values of 1 L and 0.020 L, respectively. This $V_{b10}$ value for VPN matches the desired benchmark sample volume. Furthermore, the 4-EP reached saturation within just 0.3 L, indicating a minimal amount of retention. Breakthrough of 2,5-DMF (60 ppb) was immediate and saturation was reached within 0.1 L indicating that this vapor is unretained. The VPN $V_{b10}$ value remained within 15% of the initial value after 18 breakthrough–reconditioning cycles indicating good medium-term stability of the pre-trap.

The pre-trap was then challenged with a mixture of VPN (350 ppb) and 18 other compounds ($p_v$ range = 0.00143 to 28.4 torr). Concentrations were 450 ppb for 4-EP, 50 ppb for 2,5-DMF, and from 10–15 ppb for the remaining 16 compounds. Results for 4-EP and 2,5-DMF were unaffected, but the VPN $V_{b10}$ value decreased to 0.66 L. For a sample volume of 1 L the VPN breakthrough fraction, however, was only 42% indicating that the majority of the VPN was being trapped. Given the expectation for higher capacity at lower (*i.e.*, more realistic) VPN concentrations, this level of performance was considered acceptable.

Subsequent tests were performed with and without this pre-trap installed in the instrument. A test atmosphere containing the two ETS markers and nine other vapors ($p_v$ range = 0.14 to 95 torr) was generated and aliquots injected by sample loop and flushed with 1 L of clean air. Mass-equivalent concentrations ranged from 0.9 to 200 ppb L. In all cases there was $<5\%$ reduction in detected concentrations when the pre-trap was installed compared to when it was not. An additional test series with the four SVOCs, VPN, *n*-tridecane, *n*-tetradecane, and *n*-pentadecane, added to the mixture indicated that the trapping efficiency of tridecane was 60% and those for the remaining vapors were $\geq 85\%$.

The PCF and the pre-trap were re-conditioned by heating to 300 °C with backflushing for 150 s at 0.28 L min$^{-1}$ after each of the previous samples. After 48 complete analytical cycles there was no apparent reduction in the performance of the PCF or pre-trap, and the reproducibility of peak areas for the 11-vapor mixture was better than 8% (RSD) for all vapors (based on the C8-coated CR).

## PCF

A 3 mg bed of Carbopack B challenged with 700 ppb of 4-EP in air at 0.1 L min$^{-1}$ gave a $V_{b10}$ of 3.5 L. In the presence of 18 additional vapors, each at 10–25 ppb, the 4-EP $V_{b10}$ decreased by only 0.7 L. The 4-EP desorption efficiency averaged 37 ± 2% for challenge concentrations of 1.4–18 ppb (6–72 ng), increasing to 52 ± 4% at concentrations ranging from 42–85 ppb (170–340 ng). Since no additional peaks were observed by GC-FID, we speculate that 4-EP is partially polymerizing at high temperature in the air medium within the PCF.

The 2,5-DMF, which was not retained strongly on Carbopack B ($V_{b10}$ = 0.034 L), gave a $V_{b10}$ of 6.2 L with a 3 mg bed of Carbopack X (100 ppb). No change in capacity was observed in the presence of benzene and trichloroethylene, which are the only other vapors in the 18-vapor mixture expected to pass through the Carbopack B and be trapped on Carbopack X along with 2,5-DMF.[20] A desorption efficiency of 90 ± 2% ($n$ = 3) was obtained, which was independent of mass loading from 0.78–13.1 ppb L (3–42 ng).

Estimates of preconcentration factors can be derived under the assumption that the vapors were captured from a 1 L sample volume, and that the entire desorbed mass is contained in the volume of the eluting peaks. The latter is estimated by multiplying the peak width (baseline) by the desorption flow rate. Since peak widths are measured after elution, the preconcentration factor is reduced by any peak dispersion incurred during transport through the system, and thus is a conservative, but practical, estimate. Using this approach, effective preconcentration factors for 2,5-DMF and 4-EP averaged ~4800 and ~1800 at a desorption flow rate of 1.7 mL min$^{-1}$. Some dependence on concentration is observed, hence the approximate values.

## Calibration with ETS markers and interfering compounds

A set of GC conditions was established under which 2,5-DMF and 4-EP were separated from the 14 most prominent interfering compounds eluting within the same broad retention-time window as these two markers. This was more difficult than anticipated and required, ultimately, a rather unusual temperature program that held the second column at a relatively low temperature in order to separate the 4-EP from adjacent compound peaks. The 4-EP peak exhibited a long right tail, not only with the prototype instrument but also with the bench-scale GCs used in the testing described above. Pressure (stop-flow) tuning was not useful in this analysis because the 4-EP and its closest eluting co-contaminants, *n*-undecane and *n*-dodecane, were not fully separated on the first column.

The chromatograms from the CR array sensors shown in Fig. 3 represent the best separation achievable in the minimum amount of time. Peak FWHH values are <1.5 s for the first eight compounds (#1–8 in Table 2) and then get progressively broader for the later-eluting compounds due, in part, to the low temperature used for the second column. Peak widths of the early eluting compounds were similar for the sensors and for an FID used in place of the sensors, for analyses performed under similar conditions (see Fig. 4). For the later eluting compounds, sensor peaks are broader than the corresponding FID peaks, indicating that sorption kinetics in the MPN coatings on the sensors are contributory. Regardless, using

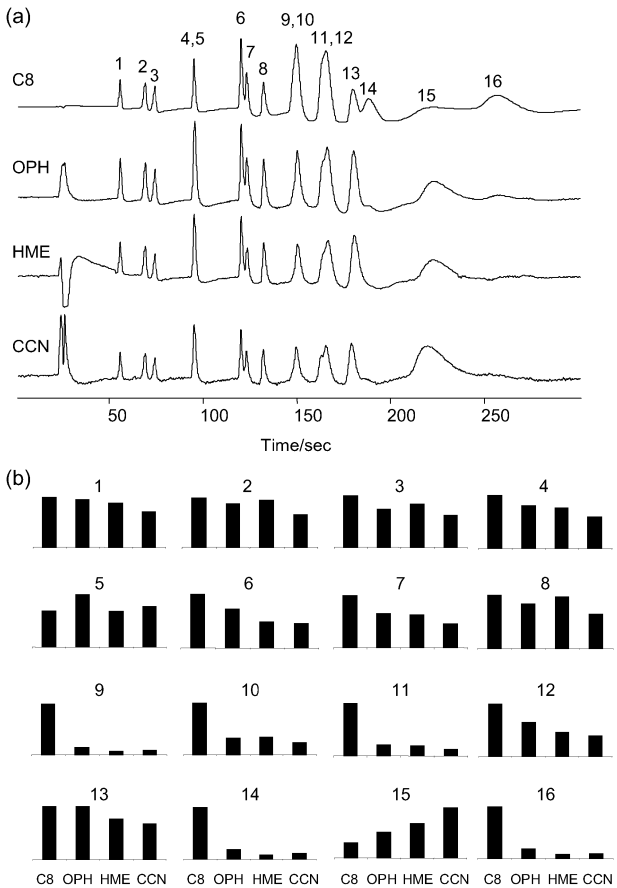


**Fig. 3** (a) CR array chromatogram traces and (b) associated response patterns of a mixture of two ETS marker compounds and 14 co-contaminants. Numbers correspond to the compounds listed in Table 2. The following temperature programs were used: column 1, 28 °C for 60 s, increase to 160 °C at 2.5 °C s$^{-1}$, hold; column 2, 55 °C, increase to 60 °C at 0.02 °C s$^{-1}$, hold. The flow rate was 1.0 mL min$^{-1}$ and the sensor array was maintained at 21.8 °C.

 

**Table 2** Calibration data summary for the 16 vapors shown in Fig. 2 (1 L sample volume)

| | | | Within-sensor relative sensitivity[a] | | | | LOD (ppb)[b] | | | | Normalized response pattern[c] | | | |
|---|---|---|---|---|---|---|---|---|---|---|---|---|---|---|
| # | Chemical | RT/s | C8 | OPH | HME | CCN | C8 | OPH | HME | CCN | C8 | OPH | HME | CCN |
| 1 | Benzene | 55 | 1.0 | 1.0 | 1.0 | 1.0 | 0.56 | 1.6 | 3.8 | 12 | 1.0 | 0.96 | 0.89 | 0.70 |
| 2 | Trichloroethylene | 68 | 1.2 | 1.3 | 1.3 | 1.2 | 0.59 | 1.8 | 3.7 | 9.8 | 1.0 | 0.88 | 0.95 | 0.67 |
| 3 | 2,5-Dimethylfuran | 73 | 1.1 | 0.89 | 1.1 | 1.0 | 0.58 | 1.9 | 4.1 | 14 | 1.0 | 0.74 | 0.83 | 0.61 |
| 4 | Toluene | 95 | 3.8 | 3.2 | 3.3 | 3.2 | 0.12 | 0.43 | 0.94 | 3.2 | 1.0 | 0.80 | 0.77 | 0.59 |
| 5 | Methyl isobutyl ketone | 95 | 2.1 | 3.2 | 2.4 | 3.4 | 0.38 | 0.55 | 1.7 | 4.0 | 0.69 | 1.0 | 0.68 | 0.78 |
| 6 | Ethylbenzene | 120 | 9.6 | 7.3 | 5.3 | 6.3 | 0.060 | 0.24 | 0.73 | 1.9 | 1.0 | 0.73 | 0.49 | 0.46 |
| 7 | *m*-Xylene | 123 | 12 | 8.2 | 8.6 | 7.9 | 0.053 | 0.21 | 0.47 | 1.6 | 1.0 | 0.65 | 0.63 | 0.46 |
| 8 | Styrene | 132 | 14 | 13 | 16 | 13 | 0.052 | 0.16 | 0.33 | 1.1 | 1.0 | 0.84 | 0.97 | 0.64 |
| 9 | *n*-Decane | 147 | 65 | 9.7 | 4.9 | 8.2 | 0.019 | 0.34 | 1.8 | 3.0 | 1.0 | 0.14 | 0.067 | 0.089 |
| 10 | 4-Ethyltoluene | 149 | 55 | 19 | 21 | 18 | 0.020 | 0.16 | 0.37 | 1.2 | 1.0 | 0.33 | 0.34 | 0.23 |
| 11 | *d*-Limonene | 162 | 104 | 22 | 23 | 18 | 0.015 | 0.18 | 0.49 | 1.6 | 1.0 | 0.20 | 0.19 | 0.12 |
| 12 | 1,2,4-Trimethylbenzene | 165 | 40 | 27 | 21 | 23 | 0.039 | 0.13 | 0.50 | 1.3 | 1.0 | 0.65 | 0.47 | 0.40 |
| 13 | 1,4-Dichlorobenzene | 178 | 41 | 43 | 36 | 40 | 0.044 | 0.098 | 0.33 | 0.79 | 1.0 | 1.0 | 0.77 | 0.68 |
| 14 | *n*-Undecane | 187 | 252 | 49 | 22 | 37 | 0.011 | 0.070 | 0.17 | 1.4 | 1.0 | 0.19 | 0.077 | 0.10 |
| 15 | 4-EP | 210 | 61 | 115 | 163 | 296 | 0.085 | 0.11 | 0.18 | 0.34 | 0.29 | 0.53 | 0.70 | 1.0 |
| 16 | *n*-Dodecane | 254 | 759 | 149 | 67 | 100 | 0.0072 | 0.060 | 0.47 | 0.64 | 1.0 | 0.19 | 0.078 | 0.093 |

[a] Values of sensitivity for all vapors from each sensor have been divided by the sensitivity value for benzene. Looking column-wise shows the range of sensitivities for each sensor among the 16 test vapors; [b] LOD calculated as $3\sigma$/sensitivity, where $\sigma$ is the RMS baseline noise (smoothed *via* binomial 40 point running average with the Grams software; $\sigma$ = 2.7, 6.4, 15, and 36 mV for C8, OPH, HME and CCN, respectively) and the sensitivity is determined on the basis of peak height (rather than peak area). For those vapors with non-linear calibration curves, LODs were estimated by extrapolation of the (linear) low-concentration range; [c] Normalized response ratios, used to derive the relative response patterns in Fig. 3, were determined by dividing the peak area sensitivity of each sensor by the largest sensitivity value among the sensors in the array for each vapor.

the independent column temperature programming, the 2,5-DMF and 4-EP peaks are fully separated from the other 14 compounds in $<240$ s (280 s is required for complete elution of *n*-dodecane).

Ambient water vapor, which permeates into the Tedlar® bag containing the test atmosphere, was also detected as the earliest eluting peak (RT = 25 s) from three of the sensors in the array, with the highest responses from the sensors coated with HME and CCN MPNs which contain polar functional groups. The unusual peak shapes from these latter two sensors, indicate that the responses have exceeded the dynamic range of the sensor readout circuit.

RT values for the 16 vapors were reproducible to within 0.4% (RSD, $n$ = 30, five replicates at six concentrations). Responses from all four CR sensors were generally reproducible (RSD $<$ 10% for five replicates). The one notable exception was *n*-dodecane on the C8- and OPH-coated sensors at the lower concentrations (RSD $>$ 20%) due to the small $S/N$ ratios.

For benzene, TCE, and 2,5-DMF, calibration concentrations up to 150 ppb were tested. For the less volatile vapors, this range was reduced to 50 ppb due to the higher sensitivities exhibited toward these vapors. For the first 12 vapors listed in Table 2, plots of peak area *versus* vapor concentration were linear from the sensors coated with OPH, HME, and CCN MPNs, with most linear-regression $r^2$ values of $>0.95$ (forced zero). For the C8 sensor, the first eight of these vapors also gave linear calibration curves ($r^2 > 0.95$), but *n*-decane, 4-ethyltoluene, and *d*-limonene became non-linear above 25 ppb. For the four least volatile vapors, responses from all four sensors became non-linear at higher concentrations. Since FID responses were linear for these vapors, we believe the non-linearity arises from the slow sorption–desorption kinetics in the sensor films, which results in incomplete mass transport of the vapors into the sensor coatings as the peak passes through the detector. Peak broadening also contributes to a loss of sensitivity in the tails of the peaks and a consequent negative integration bias. The linear response range for 2,5-DMF extends to at least 150 ppb, while that for 4-EP extends to 10 ppb.

As expected for sorption–dependent sensors, sensitivity generally increases as the vapor pressure of the analyte decreases.[26,29] This is reflected in the within-sensor sensitivity values (normalized to benzene) in Table 2. This trend is consistent across all vapors for the non-polar C8-coated sensor; as shown, the sensitivity for the least volatile *n*-dodecane is 760 times that for the most volatile benzene. For the other three sensors, functional-group interactions cause some deviations from this general trend. For example, the sensitivities of the HME- and CCN-coated sensors for 4-EP are 2.4 and 3 times higher than those for *n*-dodecane, respectively, in spite of the lower vapor pressure for the alkane.

Calculated limits of detection (LODs) range from 7.2 ppt for *n*-dodecane (C8-coated sensor) to 14 ppb for 2,5-DMF (CCN-coated sensor) (Table 2). Note that the LODs do not necessarily correlate with the sensitivity values because of differences in the baseline noise for each sensor; the CCN-coated sensor had a particularly high baseline noise level, while the C8-coated sensor had very low noise. For 14 of the 16 compounds, the C8-coated CR gives the lowest LOD and the highest sensitivity. Interestingly, for 4-EP the lowest LOD is achieved with the C8-coated sensor, even though it had the lowest sensitivity for this vapor among the four sensors. The calculated LODs for 2,5-DMF and 4-EP are 0.58 and 0.08 ppb, respectively.

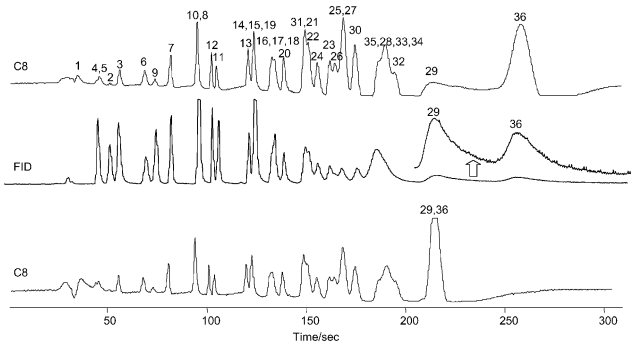


**Fig. 4** Upper trace from the C8-coated sensor shows separation of 4-EP (#29) and 2,5-DMF (#9) from 34 potential interferences in <5 min. Numbers correspond to the compounds listed in Table 1. Middle trace is from an FID used in place of the CR array for analysis of a mixture of the same compounds, excluding chloroform (inset provides enlarged view of the broad peaks for 4-EP and *n*-dodecane). Lower trace from the C8-coated sensor was obtained under conditions that accelerated the analysis; the contributions of 4-EP and *n*-dodecane to the last peak can be resolved *via* pattern recognition of the composite responses from the sensors in the array (see text).

These LODs are considered minimum values because they are based on a single sensor. If responses are needed from the entire array for vapor recognition, then the LODs increase to 14 and 0.34 ppb for 2,5-DMF and 4-EP, respectively. Compared to the earlier prototype, which employed an array of polymer-coated surface acoustic wave (SAW) sensors as the detector,[20] this instrument provides LODs that are from 20–80 times lower for the 10 compounds tested on both instruments. This can be ascribed to a combination of factors, including the higher inherent sensitivity of the CR sensors,[26,29] better thermostatting of the array, and more precise control of the temperature ramps in each separation column, which yields sharper peaks.

### Sensor array pattern recognition

In combination with the retention time, CR array response patterns provide the means to recognize eluting vapors by reference to a library of calibrated patterns. The normalized response pattern for each vapor is shown in Fig. 3 (also see Table 2). By visual inspection it is apparent that vapors from the same chemical class have patterns that are, in general, more similar than those for vapors from different classes.[26,27,38] Fortunately, chromatographic separation of homologues is relatively easy.

The 4-EP (Fig. 3, #15) response pattern is unique among the 16 prominent ETS contaminants, while the 2,5-DMF (#3) pattern resembles those of the other aromatic vapors toluene and styrene (#4 and #8) as well as that of TCE (#2). From the tabulation of relative response ratios in Table 2, the largest range of responses for any vapor is about 15-fold (*i.e.*, *n*-decane with HME- and C8-coated sensors), with typical ranges being 1.5- to 2.5-fold.

Since it is often possible to determine the contributions of the components of simple mixtures to the composite response pattern they produce, certain co-elutions can be tolerated without losing the ability to recognize the vapors.[20,39] The extent to which this is possible can be tested using Monte Carlo simulations coupled with EDPCR. From calibration, we established a library of relative response patterns to which synthetic patterns, generated by superimposing a typical amount of error on each response pattern, could be compared. Under the assumption of response additivity, composite response patterns for mixtures were created by summing the responses to the individual vapors. Iteratively generating and assigning an identity to each component of such synthetic mixture samples, over a range of concentrations from 1–5 × LOD for each vapor, yielded statistical estimates of recognition rates for the components of co-eluting mixtures.

As an example, this type of analysis was performed with each of the following three pairs of vapors, which are seen to completely co-elute in Fig. 3: toluene + methyl isobutyl ketone (#4 and #5); *n*-decane + 4-ethyltoluene (#9 and #10); *d*-limonene + 1,2,4-trimethylbenzene (#11 and #12). Results ($n$ = 500 per mixture) indicate that toluene and methyl isobutyl ketone can be recognized as components of a binary mixture at a rate of only 86%, while the components of the other two co-eluting mixture pairs can be recognized at rates of 95% and 96%, respectively. We typically apply a minimum threshold of 95% recognition to consider the determination satisfactory.[37,39] Thus, toluene and methyl isobutyl ketone would need to be chromatographically resolved for quantitative analysis, while the other pairs would not.

Focusing on the marker compounds, it turns out that there was some difficulty in separating 2,5-DMF from TCE. Monte Carlo–EDPCR analysis indicates that if these were allowed to co-elute, their recognition rate would be only 46%, highlighting the need for such separation. If the temperature program of the second column is adjusted, 4-EP can be made to co-elute with 1,4-dichlorobenzene and *n*-undecane. However, the recognition rate for this ternary mixture is only 72%. On the other hand, 4-EP could be allowed to co-elute with *n*-dodecane, since they can be recognized in the binary mixture at a very high rate of 97%. (Note: although the presence of the ETS marker could still be confirmed in many of the cases where mixture recognition was found to be low, errors in quantification are invariably incurred that lead to overestimation of the ETS marker concentration).

It is also possible to use this approach to determine if all the sensors in the array are needed for a given discrimination.[37] For the 4-EP–dodecane discrimination, additional simulations were run with various subsets of the four sensors in the array and it was found that only two sensors were required: 2-sensor arrays of C8 + CCN, C8 + HME, and OPH + CCN performed similarly, with recognition rates of >95%. Since the LOD is affected by this, one might choose the array providing the lowest LODs, which was C8 + HME for the 4-EP–dodecane case. In fact, this array provided low calculated LODs for both 4-EP (0.085 and 0.18 ppb, respectively) and 2,5-DMF (0.58 ppb and 4.1 ppb, respectively).

### Analysis of markers in a 36-component mixture

The remaining 20 vapors with $p_v > 0.1$ torr found in the field samples (Table 1) were then added to the test mixture and analyzed by the prototype instrument (less volatile vapors

 

would be captured by the pre-trap). The temperature program employed was the same as that used to separate the previous subset of compounds. The chromatogram traces from the C8-coated sensor and the FID (Fig. 4) (traces from other sensors omitted for brevity) show that 2,5-DMF and 4-EP are well separated from the 34 interfering compounds, and that the total elution time remains at 280 s. Assuming a 1 L sample volume, an entire analysis, which includes sampling, separation, detection, and post-sample purging and cooling of the PCF and pre-trap, can be completed within 16 min.

Since it was shown that 4-EP could be recognized in the presence of *n*-dodecane, the 36-component mixture was analyzed again with a sharp increase in the temperature of the second column toward the end of the elution, *i.e.*, from 58 °C to 150 °C over 9 s starting at $t = 203$ s. This reduced the retention time of *n*-dodecane by ~40 s and resulted in co-elution of the 4-EP and *n*-dodecane. The peaks were also sharpened, leading to a slight reduction of both LODs. The resulting C8 chromatogram is presented as the lower trace in Fig. 4. Thus, the separation time could be reduced by 16% (total analysis time ~15 min) by taking advantage of the capability of the sensor array to discriminate between the components of simple mixtures.

## Conclusions

The determination of two vapor-phase markers of ETS, 2,5-DMF and 4-EP (as a surrogate for 3-EP), at trace levels in complex VOC backgrounds using a uniquely equipped portable GC prototype has been demonstrated through a series of laboratory experiments. Calculated LODs and dynamic ranges for 2,5-DMF and 4-EP, assuming a 1 L sample volume, are sufficient to determine these markers in typical environmental samples.[3–10] To our knowledge this is the first reported use of a portable direct-reading instrument for this application.

Several issues related to the adaptation of this instrument to ETS-marker determinations were addressed and successfully resolved: an adsorbent pre-trap was developed to preclude SVOCs from entering the instrument and accumulating on inlet surfaces, while permitting the more volatile compounds, including the ETS markers, to pass through and be captured by the on-board preconcentrator; a two-stage preconcentrator–focuser was developed that provides quantitative trapping, high preconcentration factors, and reproducible thermal injection of markers into the separation module; independent temperature programming of the dual-column separation module was used to separate the markers from 34 interfering compounds in an elution time of <5 min; and an integrated chemiresistor array employing functionalized gold nanoparticles interface layers was used to assist in analyte recognition and to reduce the separation time. Sensor responses and GC retention times are highly reproducible and a complete sampling and analysis cycle can be completed every 15 min.

Results obtained here using the surrogate marker 4-EP are expected to be representative of those for the actual marker 3-EP. From the similarity of the GC retention times and vapor pressures reported in the literature (*vida supra*), we can infer similar capture efficiencies on the carbon adsorbents used in the PCF. It is also likely that 3-EP will exhibit relatively low recoveries upon thermal desorption in air, as observed for 4-EP, due to the inherent reactivity of the vinyl groups in both of these compounds. By analogy, with the nearly identical response patterns reported for the dimethylpyridine isomers 2,3- and 2,4-lutidine using a polymer-coated SAW sensor array,[40] we expect response patterns for 3-EP and 4-EP to be very similar as well.† Finally, since partitioning into the sensor interface layers of the CR array is governed largely by vapor pressures, the LODs for these compounds should also be similar.

## Acknowledgements

The authors wish to thank H. Wohltjen and B. Busey of Microsensor Systems, Inc. for instrument construction and invaluable technical guidance; M. P. Rowe for MPN syntheses; S. Parus for writing most of the Labview code for data acquisition; C. Jin for guidance on chemometric analyses; and C.-J. Lu for technical assistance in the early phases of the study. Primary funding was provided by Grant No. R01-OH03692 from the National Institute for Occupational Safety and Health. Additional funding was provided by Grant No. N006110 from the American Legacy Foundation. This work made use of Engineering Research Centers Shared Facilities supported by the National Science Foundation under Award Number EEC-0096866.

## References

1 International Agency for Research on Cancer, *IARC Monographs on the Evaluation of Carcinogenic Risks to Humans*, WHO Press, Geneva, Switzerland, 2002, vol. 83.
2 R. A. Jenkins, M. R. Guerin and B. A. Tomkins, *The Chemistry of Environmental Tobacco Smoke: Composition and Measurement*, Lewis Publishers, Boca Raton, FL, USA, 2nd edn, 2000, p. 49.
3 P. R. Nelson, D. L. Heavner, B. B. Collie, K. C. Maiolo and M. W. Ogden, *Environ. Sci. Technol.*, 1992, **26**(10), 1909–1915.
4 A. T. Hodgson, J. M. Daisey, K. R. R. Mahanama, J. Ten Brinke and L. E. Alevantis, *Environ. Int.*, 1996, **22**, 295–307.
5 H. R. Bohanon, J. J. Piade, M. K. Schorp and Y. Saint-Jalm, *J. Exposure Anal. Environ. Epidemiol.*, 2003, **13**(5), 378–392.
6 M. J. Hyvarinen, M. Rothberg, E. Kahkonen, T. Mielo and L. Reijula, *Indoor Air*, 2000, **10**(2), 121–125.
7 S. O. Baek and R. A. Jenkins, *Indoor Built Environ.*, 2001, **10**(3–4), 200–208.
8 M. P. Maskarinec, R. A. Jenkins, R. W. Counts and A. B. Dindal, *J. Exposure Anal. Environ. Epidemiol.*, 2000, **10**(1), 36–49.
9 B. C. Singer, A. T. Hodgson, K. S. Guevarra, E. L. Hawley and W. W. Nazaroff, *Environ. Sci. Technol.*, 2002, **36**(5), 846–853.
10 J. X. Xie, X. M. Wang, G. Y. Sheng, X. H. Bi and J. M. Fu, *Atmos. Environ.*, 2003, **37**, 3365–3374.
11 S. M. Gordon, L. A. Wallace, M. C. Brinkman, P. J. Callahan and D. V. Kenny, *Environ. Health Perspect.*, 2002, **110**(7), 689–698.
12 ASTM International, *Standard Test Method for Nicotine & 3-Ethenylpyridine in Indoor Air*, ASTM D5075-01, West Conshohocken, PA, USA, 2001.
13 C. M. Harris, *Anal. Chem.*, 2002, **74**(21), 585A–589A.

† In ref. 40, response patterns for the lutidines were nearly identical from a SAW sensor array which used a set of functionalized polymer interface layers that span a range of polarity/functionality that is comparable to that spanned by the MPN ligand functionalities used in CR array in this study. Since a high correlation is expected between mass uptake and CR resistance changes,[29] this suggests that response patterns for 4-EP and 3-EP from the CR array used as the GC detector here should be very similar.

14 G. A. Eiceman, J. Gardea-Torresdey, F. Dorman, E. Overton, A. Bhushan and H. P. Dharmasena, *Anal. Chem.*, 2006, **78**(12), 3985–3996.
15 P. A. Smith, M. T. Sng, B. A. Eckenrode, S. Y. Leow, D. Koch, R. P. Erickson, C. R. Jackson Lepage and G. L. Hook, *J. Chromatogr., A*, 2005, **1067**, 285–294.
16 Inficon Corporate home page, http://www.inficon.com, accessed June 2006.
17 X. Liu and J. Pawliszyn, *Int. J. Environ. Anal. Chem.*, 2005, **85**(15), 1189–1200.
18 J. A. Dziuban, J. Mroz, M. Szczygielska, M. Malachowski, A. Gorecka-Drzazga, R. Walczak, W. Bula, D. Zalewski, L. Nieradko, J. Lysko, J. Koszur and P. Kowalski, *Sens. Actuators, A*, 2004, **115**, 318–330.
19 L. Gao, Q. Song, G. E. Patterson, R. G. Cooks and O. Zheng, *Anal. Chem.*, 2006, **78**, 5994–6002.
20 C. J. Lu, J. Whiting, R. D. Sacks and E. T. Zellers, *Anal. Chem.*, 2003, **75**(6), 1400–1409.
21 C. J. Lu, C. Jin and E. T. Zellers, *J. Environ. Monit.*, 2006, **8**(2), 270–278.
22 Q. Zhong, W. H. Steinecker and E. T. Zellers, manuscript in preparation.
23 C. J. Lu and E. T. Zellers, *Analyst*, 2002, **127**, 1061–1068.
24 RVM Scientific Inc. home page, http://www.rvmscientific.com, accessed June 2006.
25 T. Veriotti and R. D. Sacks, *Anal. Chem.*, 2001, **73**, 814–819.
26 Q. Y. Cai and E. T. Zellers, *Anal. Chem.*, 2002, **74**, 3533–3539.
27 C. J. Lu, W. H. Steinecker, W. C. Tian, M. Agah, J. M. Potkay, M. C. Oborny, J. Nichols, H. Chan, J. Driscoll, R. D. Sacks, S. W. Pang, K. D. Wise and E. T. Zellers, *Lab Chip*, 2005, **5**, 1123–1131.
28 M. P. Rowe, K. E. Plass, K. Kim, C. Kurdak, E. T. Zellers and A. J. Matzger, *Chem. Mater.*, 2004, **16**, 3513–3517.
29 W. H. Steinecker, M. P. Rowe and E. T. Zellers, *Anal. Chem.*, submitted.
30 EPA TO-17, *Compendium of Methods for the Determination of Toxic Organic Compounds in Ambient Air*, Report No. EPA/625/R-96/010b, US Environmental Protection Agency, Washington, DC, 2nd edn, 1997.
31 C. Jia, S. Batterman and S. Chernyak, *J. Environ. Monit.*, 2006, **8**(2), 1029–1042.
32 P. H. Howard and W. M. Meylan, *Handbook of Physical Properties of Organic Chemicals*, Lewis, New York, 1997.
33 *CRC Handbook of Chemistry and Physics, Internet Version 2005*, ed. D. R. Lide, CRC Press, Boca Raton, FL, USA, 2005, pp. 3–568, http://www.hbcpnetbase.com.
34 C. N. Davies, *Ann. Occup. Hyg.*, 1985, **29**, 13–25.
35 C. J. Lu and E. T. Zellers, *Anal. Chem.*, 2001, **73**, 3449–3457.
36 E. T. Zellers, S. A. Batterman, M. Han and S. J. Patrash, *Anal. Chem.*, 1995, **67**, 1092–1106.
37 J. Park, W. A. Groves and E. T. Zellers, *Anal. Chem.*, 1999, **71**, 3877–3886.
38 C.-Y. Yang, C.-L. Li and C.-J. Lu, *Anal. Chim. Acta*, 2006, **565**, 17–26.
39 M. D. Hsieh and E. T. Zellers, *Anal. Chem.*, 2004, **76**, 1885–1895.
40 S. Patrash and E. T. Zellers, *Anal. Chem.*, 1993, **65**, 2055–2066.


 